

X-FEM 2D crack propagation under rolling contact fatigue taking into account realistic residual stresses

Benoit Trolle^{1,2}, Marie-Christine Baietto¹, Anthony Gravouil^{1,3}, Si Hai Mai², Benoit Prabel⁴, Mac-Lan Nguyen-Tajan²

¹ Laboratoire de Mécanique des Contacts et des Structures (LaMCoS), INSA de Lyon, CNRS UMR 5259, Bat. Jacquard, 18-20 rue des sciences, F69 621 Villeurbanne Cedex, benoit.trolle@insa-lyon.fr.

² SNCF, Innovation & Research Department, 40 avenue des Terroirs de France, 75611 Paris Cedex 12, benoit.trolle@sncf.fr.

³ Institut Universitaire de France.

⁴ CEA, DEN/DM2S/SEMT/DYN, CE-Saclay, 91191 Gif-sur-Yvette Cedex, France.

ABSTRACT. *Due to the repeated passages of the wheels, rolling contact fatigue cracks can appear in the surface or subsurface of the rails. These defects can propagate and lead to the rail failure. A two-scale frictional contact fatigue crack model developed within the X-FEM framework is used to solve the crack problem. Realistic residual stresses, coming from dedicated software developed by SNCF are introduced in the propagation simulation via projection of the asymptotic mechanical fields. Crack growth is performed taking into account this permanent non-uniform field. Results show that SIFs ratio is modified by those residual stresses influencing the crack propagation path.*

INTRODUCTION

The numerical crack growth in tribologic fatigue is a large research topic which involves the understanding and the modelling of numerous local phenomena like confined plasticity or interfacial frictional contact. Contact with friction between the crack faces notably occurs in rolling contact fatigue problems. These possible time-dependent, multi-axial, non proportional loadings may lead to crack, up to the development of very complex 3D crack network. These defects, such as squats and head-checks, lead to the rail failure and potentially to a derailment. Costly maintenance operations are deployed to avoid such a situation.

To improve the understanding of the crack initiation and propagation mechanisms, a numerical modelling tool has been developed thanks to a long-term collaboration between French railway organizations (SNCF, RATP, RFF), rail producer (Tata Steel) and research institutes and universities (LaMCoS/INSA Lyon,

MS/Polytechnique, MECAMIX, IFSTAR) within the consortium IDR2 (Initiative for Development and for Research on Rails). The first step of this modelling tool deals with a railway multi-body dynamics simulation to give contact conditions at the wheel-rail interface. In the next step, the cyclic mechanical state of the rail is calculated by means of a 3D finite element simulation and an original, time-cost efficient direct stationary algorithm. Then, a fatigue analysis of the rail is performed with the DangVan criterion. The final step consists of modelling the crack growth. This paper focuses on this last point: modelling fatigue crack growth in the rails taking into account frictional contact between the crack faces, mixed-mode propagation and realistic residual stresses.

Model the crack propagation under rolling contact fatigue (RCF) requires taking into account different phenomena acting on different scale. At the structure scale, the wheel-rail contact imposes a very high gradient close to the wheel-rail contact area and lead to a multi-axial non-proportionnal loading of the cracks. Moreover the repeated traffic of the wheel over the rail leads to an asymptotic stresses in the rail that will influence the crack propagation. All these solicitations imply complexe sequences of opening, sticking and sliding conditions at the crack scale.

Previous works about fatigue crack growth in the rails are available in the literature. Some authors have studied the role of liquid entrapment using FEM analysis [1,2,3] or BEM analysis [4,5] in the crack growth mechanism. This effect is not considered in this work. Other works have studied the influence of different parameters such as elastic foundation [6], the crack initial geometry [6,7,8,9] or the crack face friction coefficient [6,8,9,10] on the stress intensities factors (SIFs). In this paper we present 2D results of fatigue crack growth in the rails taking into account realistic residual stresses using a two-scale X-FEM/LATIN crack model with interfacial frictional contact.

TWO-SCALE CRACK MODEL WITH INTERFACIAL FRICTIONAL

We consider a cracked body $\Omega \in \mathbb{R}^3$ where contact and friction can occur along the crack faces Γ_C^+ and Γ_C^- . Under small displacement and small strain assumptions, we assume the interface $\Gamma_C = \Gamma_C^+ \cup \Gamma_C^-$ as an autonomous entity with its own behavior possibly nonlinear. This fracture problem is divided in a global problem (structure scale $\Omega \setminus \Gamma_C$) and a local problem (crack scale Γ_C) (see Fig. 1). The global problem is defined with its own primal and dual variables, u the displacement field and σ the Cauchy stress tensor respectively. The local problem is defined with its own primal and dual variables, w is the interface displacement field and f is the interface traction field respectively. Let n be the outward unit normal to $\Omega \setminus \Gamma_C$ and n_C is the outward unit normal to Γ_C . We assume quasi-static formulation and write the governing equations as follows for the global problem at a given time $t \in [0; T]$:

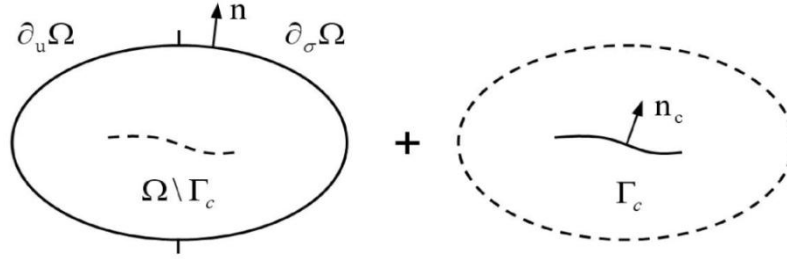


Figure 1. Cracked body problem divided into a global problem and a local interface problem.

Using the principle of virtual work we can write the work of the uncracked body, the interface problem and the coupling work and obtain a three weak field formulation of the problem. Details can be found in [11]:

$$P_{\Omega \setminus \Gamma_c}^* + P_{\Gamma_c}^* + P_{\text{coupling}}^* = 0 \quad \forall (u^*, w^*, f^*) \text{ admissible} \quad (1)$$

This formulation (Eq. 1) has been stabilised [12] to avoid numerical instabilities.

At the local scale governing equations are the unilateral contact and Coulomb's law:

$$\text{opening} \quad [w_N(x, t)] > 0 \rightarrow f^+(x, t) = f^-(x, t) = 0 \quad (2)$$

$$\text{contact} \quad [w_N(x, t)] = 0 \rightarrow f^+(x, t) = -f^-(x, t) \quad (3)$$

$$\text{sticking} \quad |f_T(x, t)| < \mu_C |f_N(x, t)| \rightarrow \Delta[w_N(x, t)] \quad (4)$$

$$\text{sliding} \quad |f_T(x, t)| = \mu_C |f_N(x, t)| \rightarrow \exists \gamma > 0 / \Delta[w_N(x, t)] = -\gamma f^+(x, t) \quad (5)$$

X-FEM DISCRETIZATION AND NON-LINEAR SOLVER DEDICATED TO INTERFACIAL FRICTIONAL CONTACT

The eXtended Finite Element Method [13] is used to model the crack propagation. In this method no explicit representation of the crack is needed. The crack is modelled using function enrichments. The crack discontinuity is introduced as a Heaviside step function. In addition, branch functions are introduced for all elements containing the crack front. Hence, the mesh does not necessarily conform to the crack and both field interpolation and remeshing are not required during the possible crack propagation.

One assumes that the state vector $X_n = (u_n, w_n, f_n)$ is known at time t_n . Within a quasi-static incremental framework, the next stage consists of calculating the unknown state vector X_{n+1} at time step t_{n+1} . The LATIN method consists of an iterative strategy between a local stage from X_n^i to $X_n^{i+\frac{1}{2}}$ and a global stage from $X_n^{i+\frac{1}{2}}$ to X_n^{i+1} . The local stage corresponds to a set of local equations ((L) on Fig. 2), possibly non linear (Eqs. 2, 3, 4 and 5), and the global stage to a set of global linear equations ((G) on Fig.2) (see (17)). This two-step approach requires search directions E^+ and E^- between the set of equations (L) and (G) (see Fig. 2). The process is repeated until convergence is reached. The iterative process has been recently optimized to obtain the best convergence rate possible [14].

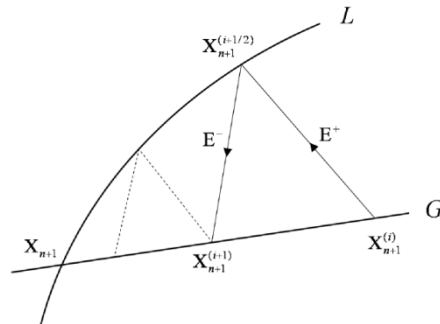


Figure 2. Schematic representation of the LATIN method.

INTRODUCTION OF REALISTIC RESIDUAL STRESSES

The evaluation of the mechanical state in the rail due to the contact stress induced by the railway traffic is crucial for the modeling of the rail resistance: plastic deformations occur in the region near the contact zone due to repeated rolling– sliding contacts between the wheels and the rail. To be realistic, it is necessary to take into account this phenomenon which may be very significant for crack initiation and propagation in the rail head. It is well known that under repeated rolling contacts, different asymptotic mechanical states could occur in the structure: elasticity, elastic shakedown, plastic shakedown or ratcheting.

Determination of the stabilized state in the rail is performed by using sequentially VOCOLIN software [16] and the stationary algorithm [17]. First, the contact between wheel and rail is evaluated by means of VOCOLIN. Its characteristics, which are number and dimensions of contact areas, normal and tangential pressure, can be Hertzian or non-Hertzian (se Fig. 3(a)). Then, using the stationary algorithm, the stabilized mechanical state (residual stresses and plastic strain distribution) is computed. An elastic shakedown is obtained (Fig. 3(b)); all components of the plastic deformation tensor are constant along all the streamlines of the gauge corner. As a consequence, high cycle fatigue is likely to occur.

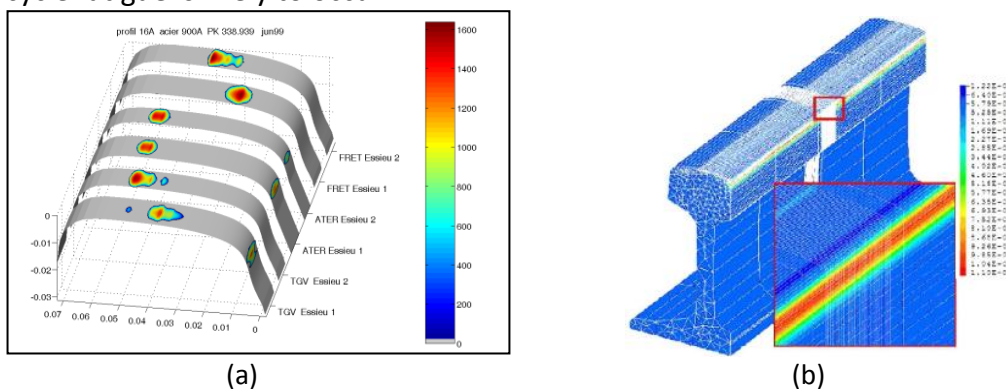


Figure 3. (a) Examples of calculated rail/wheel contact area obtained by simulation (VOCOLIN). (b) Stabilized longitudinal plastic strain distribution [15].

The asymptotic mechanical fields are then projected on the mesh used to model the crack propagation (see Fig. 4). Those fields are considered as the initial state of the propagation simulation. This state is permanent and non-uniform. No redistribution of residual stresses is considered throughout the crack growth. Since only elastic shakedown is considered the fields after projection do not required to be re-balanced.

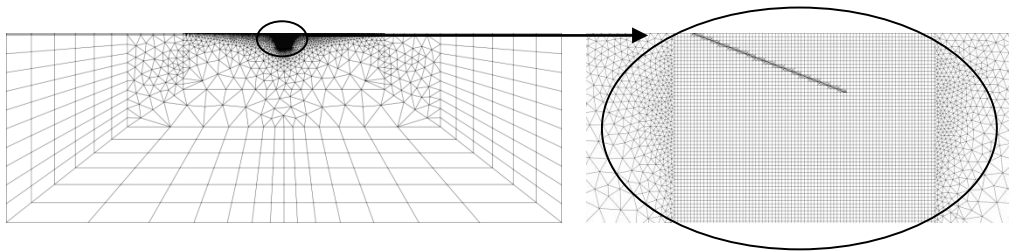


Figure 4. Example of 2D-mesh used to model the crack propagation.

CRACK GROWTH UNDER PROCEDURE ROLLING CONTACT FATIGUE

A wheel passage on the rail corresponds to a loading cycle for a crack in the rail. In The propagation simulation, whee-rail contact is modeled as a fully sliding herzian load. Each cycle is divided in time step corresponding to the position of the wheel with respect to crack. For each position of the wheel, the crack body problem is solved and SIFs are computed using integral methods. At the end of a simulated cycle, we have the history of SIFs throughout the cycle. Using this history, the crack growth path (direction) is here predicted according to Hourlier and Pineau's criterion already validated under non-proportional loading [18]. Finally a dedicated mixed-mode propagation is used to predict the crack crack growth rate [9]. In the end of the cycle the new crack is created and the corresponding jump cycle is computed thanks to the propagation law. The procedure is repeated until no more cycles are required (Fig. 5).

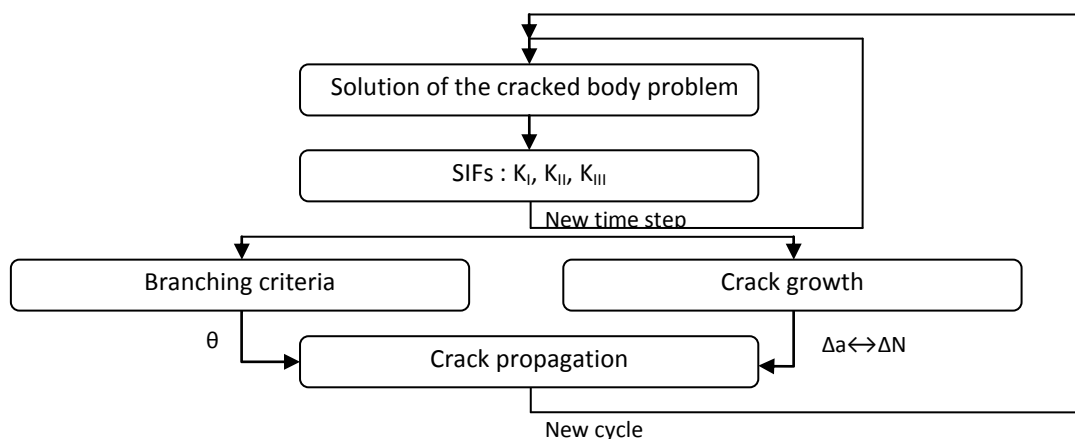


Figure 5. Flow charts of the propagation procedure.

Determination of the suitable Hourlier and Pineau criteria

Hourlier and Pineau criteria are actually three different criteria. [18] has already shown that $\max \Delta k_1^*$, $\max \Delta k_1^*(\theta, t)$ and $\max \frac{da}{dn}(\theta, t) = f(k_1^*, k_2^*)$ are suitable criteria for fretting-fatigue problems. The same conclusions are here derived (Fig. 7 (b)) from the following test case (Fig. 6). The maximal pressure is 845 Mpa, the contact patch dimension $2a$ is 13.5mm and the initial crack is 1mm long inclined with an angle of 45° with the upper rail surface. The crack friction coefficient is 0.1 and the friction coefficient between the wheel and the rail is set to 0.4. 92 time steps of 0.25mm are considered. The crack in the initial configuration intersects 27 elements of the mesh.

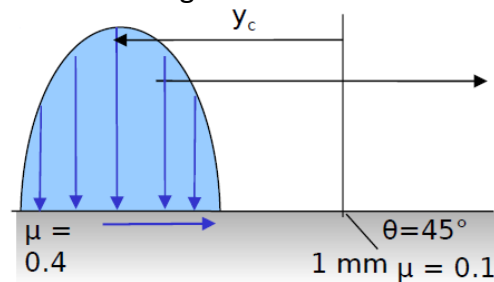


Figure 6. Reference problems

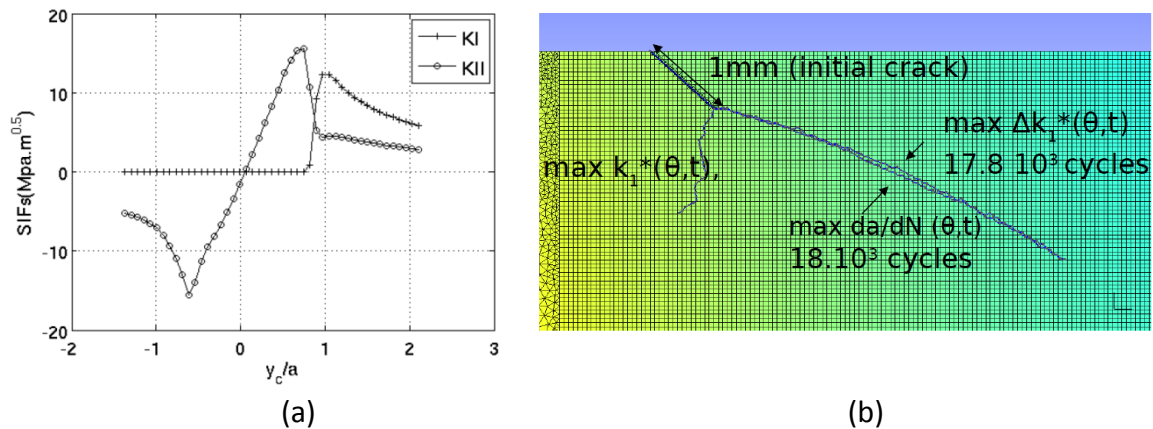


Figure 7. (a) SIFs history after the initial cycle, (b) Crack propagation path using the three different Hourlier and Pineau Criteria.

We can see on the Fig. 7 (b) that two of the criteria predict the same crack growth path with the same crack growth rate. The $\max k_1^*$ criterion gives a different path. This criterion is based on a similar approach than the maximal tangential stress criterion, they are both based on maxima over a cycle. But since the loading is non-proportionnal this approach is not suitable for propagation under RCF. Hence we use the two others criteria to predict the crack growth path in the study.

Results with simplified residual stresses

We now first introduced simplified residual stress via external loading on the sides of the domain (Fig. 8 (a)).

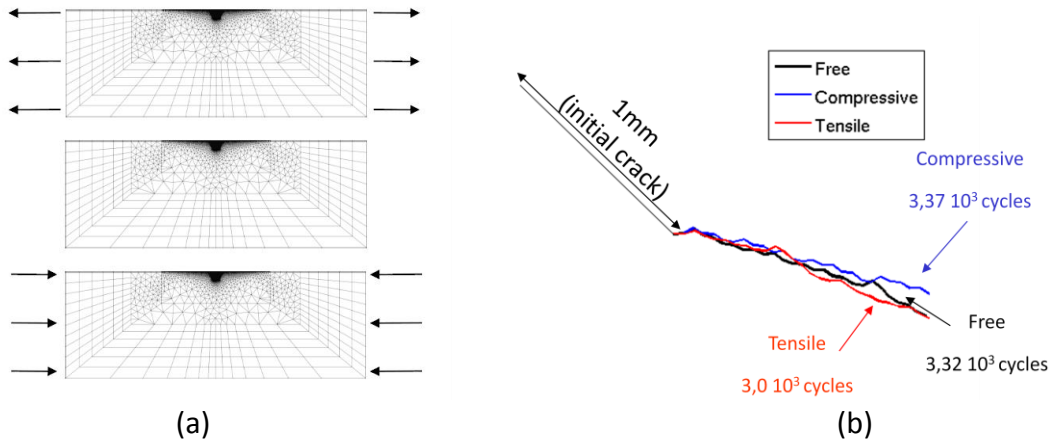


Figure 8. Introduction of simplified residual stresses in the model (a) and results (b)

No influence on the crack growth is observed in this case (Fig 8. (b)). It has to be point out that the crack is still short in comparison with the wheel-rail contact patch and therefore the driving force of the propagation is still the contact stresses imposed by the wheel. It still can be noticed differences on the crack growth rate.

Preliminary results with realistic residual stresses

Preliminary studies with realistic residual stresses have been performed. In this test case, the crack is vertical and always opened. It has shown that with realistic residual stress field, the ratio K_I/K_{II} along the cycle is modified leading to a modification of the crack propagation.

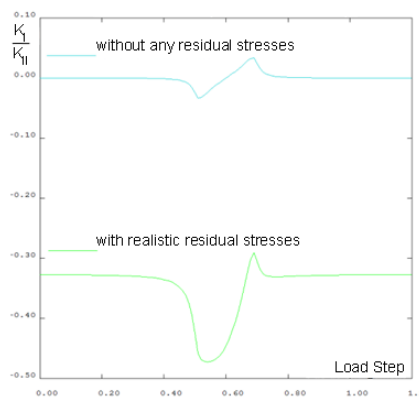


Figure 9. Modification of the K_I/K_{II} ratio with realistic residual stresses.

CONCLUSION

This paper aims at predicting fatigue crack growth and branch conditions under RCF. A two-dimensional linear elastic numerical model for fatigue crack growth has been presented including contact with friction at crack interface. The model rests on a three weak field formulation using X-FEM and an iterative scheme dedicated to non-linear interface problems adapted from the LATIN method. Using the tools already developed by SNCF to solve the wheel-rail contact problem and to compute the asymptotic stresses in the rail, realistic residual stresses has been introduced in the propagation model assuming elastic shakedown for the rail. Specific branching criteria and propagation law dedicted to non proportional loading and RCF has been used. First results show that the $\max \Delta k_I^*(\theta, t)$ criterion and the $\max \frac{da}{dn}(\theta, t)$ criterion are suitable for RCF. Preliminary results have shown that using simplified residual stresses, the residual stresses influence the crack growth rate and finally introducing realistic residual stresses that the ratio K_I/K_{II} is modified and will lead to a different crack growth path.

REFERENCES

1. Bogdanski S. (2005) *Wear* **258**, 1273–1279.
2. Bogdanski S. (2008) *Wear* **265**, 1356–1362.
3. Farjoo M., Pal S., Daniel W., Meehan P.A. (2012) *Eng. Fract. Mech.* **94**, 37–55.
4. Fletcher D.I., Hyde P., Kapoor A. (2007) *Rail Rapid Transit* **221(1)**, 35-44.
5. Fletcher D.I., Hyde P., Kapoor A. (2008) *Wear* **265**, 1317–1324.
6. Farjoo M., Pal S., Daniel W., Meehan P.A. (2012) *Eng. Fract. Mech.* **85**, 47-58.
7. Seo J., Kwon S., Jun H., Lee D. (2010) *Procedia Eng.* **2**, 865-872.
8. Brouzoulis J., Ekh M. (2012) *Int. Jnl. of Fatigue* **45**, 98–105.
9. Dubourg M.-C. , Lamacq V. (2002) *Jnl. of. Tribol.* **124**, 680-688.
10. Fletcher D.I., Smith L., Kapoor A. (2009) *Eng. Fract. Mech.* **76**, 2612–2625.
11. Ribeaucourt R., Baietto-Dubourg M.-C., Gravouil A. (2007) *Comput. Meth. Appl. Mech. Eng.* **196**, 3230–3247.
12. Gravouil A., Pierres E. , Baietto M.-C. (2011) *Int. J. Numer. Meth. Engng.* **88**, 1449-1475.
13. Moës N., Dolbow J., Belytschko T. (1999) *Int J. Numer. Meth. Engng.* **46**, 131-150.
14. Trollé B., Gravouil A., Baietto M.-C, Nguyen-Tajan T.M.L. (2012) *Finite Elem. Anal. Des.* **59**, 18-27.
15. Dang Van K., Maitournam M.H., Moumni Z., Roger F. (2009) *Eng. Fract. Mech.* **76** 2626–2636.
16. Ayasse J.B., Chollet H. (2005) *Vehicle Syst. Dynam.* **43(3)**, 161-72.
17. Dang Van K., Maitournam M.H (1993) *J. Mech. Phys. Solids* **41(11)**, 1691-1710.
18. Baietto M.C., Pierres E., Gravouil A., Berthel B., Fouvry S, Trolle B. (2013) *Int. Jnl. of Fatigue* **47** 31-43.